Available online at www.sciencedirect.com
ScienceDirect
Journal of Sound and Vibration 315 (2008) 985–1002
JOURNAL OF SOUND AND VIBRATION
www.elsevier.com/locate/jsvi

Three-port impedance model of a piezoelectric bar element: Application to generation and damping of extensional waves

A. Jansson, B. Lundberg*

The Ångström Laboratory, Uppsala University, Box 534, SE-751 21 Uppsala, Sweden

Received 15 August 2007; received in revised form 26 January 2008; accepted 11 February 2008
Handling Editor: C. L. Morfey
Available online 18 April 2008

Abstract

A straight bar element containing piezoelectric members is viewed as a linear system with one electrical and two mechanical ports where it can interact with external electrical and mechanical devices through voltage, current, forces and velocities. A generalized force vector, with one voltage and two forces as elements, is expressed as the product of an impedance matrix and a generalized velocity vector, with one current and two velocities, as elements. Due to symmetry and reciprocity, this matrix is defined by four of its nine elements. Two applications are considered for a piezoelectric bar element (PBE) that constitutes a part of a long elastic or viscoelastic bar, viz. generation and damping of extensional waves in the bar. In the first, the PBE is driven by a given input voltage or by the output voltage from a linear power amplifier. In the second, the PBE supplies an output voltage to an external load. In numerical simulations carried out for a specific laminated PBE, an elastic bar, a serial RL load and a bell-shaped incident wave, the highest fraction of wave energy dissipated was 8.1%. This is much less than the 50% achievable for a harmonic wave under condition of electrical impedance matching.

1. Introduction

Piezoelectric members in the form of thin plates, covered with conducting electrode layers, are increasingly used as sensors, e.g. [1,2], and actuators, e.g. [3,4], in different applications. Their ability of producing electrical output when subjected to mechanical input, and vice versa, can be derived from two coupled constitutive equations of the piezoelectric materials [5]. These equations relate the mechanical and electrical fields and are known as the sensor and actuator equations. The piezoelectric members have large bandwidth and are suitable for integration in host structures.

The interactions of piezoelectric members with passive and active electrical devices and with host structures give rise to a multitude of phenomena. The analyses of such interactions and phenomena generally involve the full constitutive behaviour of the piezoelectric materials, and also the dynamics of the piezoelectric members, the electrical devices and the host structures. Often, not all of these ingredients are important. If, e.g., an

*Corresponding author.
E-mail address: bengt.lundberg@angstrom.uu.se (B. Lundberg).

0022-460X/$ - see front matter © 2008 Elsevier Ltd. All rights reserved.
doi:10.1016/j.jsv.2008.02.013

Nomenclature

Latin

A	cross-sectional area
c	wave speed
C	capacitance
d	piezoelectric constant
D	electric displacement
e	strain
E	Young's modulus
f	frequency
G	voltage gain of unloaded amplifier
h	height
i	current
i	unit of imaginary numbers
k	square root of electromechanical coupling coefficient
K	stiffness
l	length
L	inductance
N	normal force
P	power
Q	charge
R	real part of impedance, resistance
t	time
U	voltage
v	particle velocity
w	normalized energy, width
W	energy
X	imaginary part of impedance
x	axial coordinate
y	transverse coordinate (horizontal)
z	transverse coordinate (vertical)
Z	impedance (mechanical, electrical, or mixed)
$\mathbf{Z}$	impedance matrix

Greek

γ	wave propagation coefficient
ε	permittivity
ρ	density
ω	angular frequency

Superscripts

av	average
DC	direct current
E	electrical
M	mechanical

Subscripts

0	electrical port
1	1st mechanical port
2	2nd mechanical port
a	piezoelectric layer
b	bonding layer
c	core layer
ch	characteristic
D	dissipated
G	generated
I	incident
in	input
int	internal
n	direction of decreasing x
p	direction of increasing x
R	reflected
T	transmitted
tr	transit

actuator is driven by an amplifier with output impedance that is low enough relative to the load impedance, the sensor equation may be immaterial. If, in addition, the bandwidth of the amplifier is large enough, its dynamics may be neglected. Also, if the transit time of mechanical waves through a piezoelectric member is sufficiently small compared with relevant characteristic times, the member may be considered as quasi-static. Such simplifications were natural in the early work by Crawly and de Luis [6] on the interaction of piezoelectric actuators and beams, which, however, included the effect of shear deformation in the bonding layers.

Actuator dynamics was taken into account, e.g., by Pan et al. [7] in the study of an Euler–Bernoulli beam with perfectly bonded piezoelectric actuators (i.e., no shear deformation in the bonding layers). They showed that the dynamics of the actuators has significant influence on the response of the beam, especially at locations close to the actuators and when the driving frequency does not correspond to a resonance frequency of the beam. Allowance for the interaction of the host structure and electrical circuits through the piezoelectric effect, and for the two coupled constitutive equations, was made by Hagood et al. [8]. They applied a generalized form of Hamilton's principle to an elastic structure containing piezoelectric elements connected to an electrical

circuit with embedded voltage and current sources and specialized their results to a cantilever beam. Similar considerations have been made by others [9–13], in particular by Thornburgh and Chatopadhyay [9] and Thornburgh et al. [10] who used a variational approach based on Hamilton's principle and derived results for cantilever plates.

While much published work on piezoelectricity concerns harmonic vibrations of beams and plates, only little such work deals with transient extensional waves in bars. A model for generation of such waves in a linearly elastic or viscoelastic bar by use of a perfectly bonded piezoelectric actuator pair driven by a linear power amplifier was developed in a preceding paper [14]. This model, which allows for the coupled constitutive equations and for the dynamics of the actuators, the amplifier and the bar, is essentially an extensional analogue of the model for flexural vibrations used in Ref. [8]. The problem of finding the input voltage to the amplifier required for generation of a prescribed wave output was considered, and in a subsequent experimental study [15] good agreement was obtained between implemented and prescribed waves in an elastic bar. This problem is of interest in control applications, such as Ref. [16], where waves prescribed on the basis of information from sensors are used to cancel disturbing waves.

In this paper, a straight bar element containing axially oriented piezoelectric members is viewed as a linear system with one electrical and two mechanical interfaces or ports. The element can interact with an external electrical device at the electrical port and with external mechanical devices at the mechanical ports. These interactions are described in terms of a voltage and a current at the electrical port and a force and a velocity at each mechanical port. The voltage and the two forces are considered as generalized forces, and the current and the two velocities as generalized velocities. Because of assumed linearity, the vector of generalized forces can be expressed as the product of an impedance matrix and the vector of generalized velocities. Due to assumed symmetry and reciprocity, this impedance matrix is defined by four of its nine elements. Once these four impedance elements of the piezoelectric bar element (PBE) have been determined, it is straight-forward to analyze its function as an actuator or a sensor in different environments of electrical and mechanical devices.

In Section 2, the three-port impedance model of the PBE will be presented. First, the general case will be considered. Then the four independent elements of the impedance matrix will be determined for the specific laminated PBE employed in the preceding theoretical [14] and experimental [15] studies of extensional wave generation and in a parallel experimental study [17] of extensional wave damping. In Section 3, the PBE will be considered a part of a long bar, the external parts of which are elastic or viscoelastic, and generation of extensional waves will be studied when the PBE is driven either with a given voltage or with the output voltage of a linear amplifier with finite output impedance. In Section 4, the same assembly of PBE and bar will be considered, but here damping of extensional waves will be studied when the electrical port is shunted by an external impedance load. In both Sections 3 and 4, the results obtained for a general PBE will be specialized to the specific laminated one. Finally, the results will be discussed in Section 5, and the main conclusions will be summarized in Section 6.

2. Three-port impedance model

2.1. General case

Consider a straight bar element containing axially oriented piezoelectric members, either on the surface or embedded into linearly elastic or viscoelastic materials. The element is assumed to be sandwiched between external mechanical devices with which it can interact. In particular, the element may constitute a part of a single straight bar. In this case, the external mechanical devices are the parts of the bar external to the element itself. The electromechanical response of the piezoelectric members is assumed to be linear.

The PBE considered is illustrated in Fig 1(a), where x is a coordinate along its axis, and y and z are transverse coordinates. The PBE and the external mechanical devices are assumed to be symmetric with respect to the planes xy and xz. In addition, the PBE is assumed to be symmetric with respect to the plane yz. These symmetries of the PBE concern its geometrical, mechanical and electrical properties.

The piezoelectric members are assumed to be interconnected in such a way that the PBE can interact with external active or passive electrical devices at a single interface or port labelled 0. At this electrical two-terminal port, the voltage is $\hat{U}_0(\omega)$ and the current is $\hat{i}_0(\omega)$, where ω is the angular frequency. As shown in the

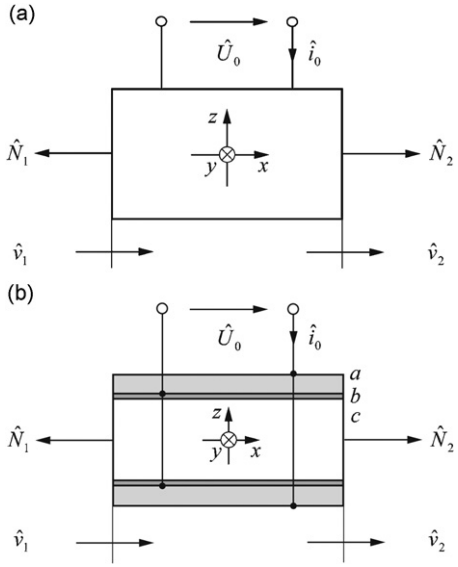

Fig. 1. Three-port representation of (a) general PBE and (b) laminated PBE.

figure, the current is defined as positive in the direction it would be driven through the port by a positive voltage applied externally. Here and below, the notation $\hat{\phi}(\omega)$ is used for the Fourier transform of a function $\phi(t)$ of time t assumed to be piecewise differentiable and absolutely integrable.

The PBE can interact with external active or passive mechanical devices at two interfaces or ports constituted by its ends. They are perpendicular to the bar axis and are labelled 1 and 2. At these mechanical ports the normal forces are $\hat{N}_1(\omega)$ and $\hat{N}_2(\omega)$, and the velocities are $\hat{v}_1(\omega)$ and $\hat{v}_2(\omega)$. As shown, the forces are defined as positive in tension and the velocities in the direction of the x-axis. Generalized forces and velocities related to bending or torsion are assumed not to be generated by the PBE, by the external devices or by their interaction.

The power supplied to the PBE at the different interfaces is $U_0 i_0$, $N_1(-v_1)$ and $N_2 v_2$. Therefore, $\hat{U}_0$, $\hat{N}_1, \hat{N}_2$ and $\hat{i}_0, -\hat{v}_1, \hat{v}_2$ are chosen as generalized forces and velocities, respectively. Because of assumed linearity, the generalized forces are related to the generalized velocities by

$$\begin{bmatrix} \hat{U}_0 \\ \hat{N}_1 \\ \hat{N}_2 \end{bmatrix} = \begin{bmatrix} Z_{00} & Z_{01} & Z_{02} \\ Z_{10} & Z_{11} & Z_{12} \\ Z_{20} & Z_{21} & Z_{22} \end{bmatrix} \begin{bmatrix} \hat{i}_0 \\ -\hat{v}_1 \\ \hat{v}_2 \end{bmatrix}, \tag{1}$$

where $Z_{00}(\omega), Z_{01}(\omega), \ldots, Z_{22}(\omega)$ are the elements of a 3×3 impedance matrix $\mathbf{Z}(\omega)$. This matrix has the property $\mathbf{Z}(-\omega) = \overline{\mathbf{Z}}(\omega)$, where $\overline{\mathbf{Z}}$ denotes the complex conjugate of $\mathbf{Z}$. Thus, real and imaginary parts of $\mathbf{Z}$ are even and odd functions, respectively, of ω.

By the assumption of reciprocity, the impedance matrix is symmetric and therefore

$$Z_{10} = Z_{01}, \quad Z_{20} = Z_{02}, \quad Z_{21} = Z_{12}. \tag{2a–c}$$

Because of the symmetry with respect to the plane yz, the subscripts 1 and 2 are interchangeable and therefore

$$Z_{02} = Z_{01}, \quad Z_{20} = Z_{10}, \quad Z_{22} = Z_{11}. \tag{2d–f}$$

As far as its electrical and mechanical interactions with external devices are concerned, the PBE can be represented by the impedance matrix $\mathbf{Z}$ defined by the four elements Z_{00}, Z_{01} ($= Z_{10} = Z_{20} = Z_{02}$), Z_{11} ($= Z_{22}$) and Z_{12} ($= Z_{21}$). The nature of Z_{00} is electrical, that of Z_{01} is electromechanical and that of Z_{11} and Z_{12} is mechanical. The units of these impedances are V/A $= \Omega$, N/A $=$ Vs/m and Ns/m, respectively.

Consider now a PBE with imaginary impedance matrix, $Z_{ij} = \mathrm{i}X_{ij}$. Also, let the generalized forces and velocities be harmonic with angular frequency ω and interpret $\hat{U}_0, \hat{N}_1, \hat{N}_2$ and $\hat{i}_0, -\hat{v}_1, \hat{v}_2$ as complex effective amplitudes. Then, the total average power $P = \mathrm{Re}[\hat{U}_0\bar{\hat{i}}_0 + \hat{N}_1(-\bar{\hat{v}}_1) + \hat{N}_2\bar{\hat{v}}_2]$ supplied to the PBE at its three ports can be shown to be zero. Therefore, an imaginary impedance matrix represents a PBE that is lossless.

In the absence of piezoelectricity, the elements of the impedance matrix become $Z_{\mathrm{ij}} = Z'_{\mathrm{ij}}$ with the electromechanical coupling elements zero, i.e., $Z'_{01} = Z'_{10} = Z'_{02} = Z'_{20} = 0$. Therefore, Eq. (1) splits up into the two uncoupled relations

$$\hat{U}_0 = Z'_{00}\hat{i}_0, \quad \begin{bmatrix} \hat{N}_1 \\ \hat{N}_2 \end{bmatrix} = \begin{bmatrix} Z'_{11} & Z'_{12} \\ Z'_{21} & Z'_{22} \end{bmatrix} \begin{bmatrix} -\hat{v}_1 \\ \hat{v}_2 \end{bmatrix}. \tag{3a,b}$$

Next, it will be shown for a specific laminated PBE how the elements of the impedance matrix $\mathbf{Z}$ depend on the geometry and the materials. Such a PBE, serving as an actuator, was studied theoretically with a different approach in Ref. [14]. In that study, the properties of the PBE itself, isolated from its mechanical and electrical environment, were not considered as here. It was investigated experimentally in Ref. [15].

2.2. Specific case

Consider the specific laminated PBE shown in Fig. 1(b). Two piezoelectric layers a are attached to each side of a core c by bonding layers b, all of the same length l. The cross section of each layer is rectangular and the full cross section is symmetric with respect to the y and z axes. The layers have heights h_a, h_b and h_c, widths w_a, w_b and w_c, and cross-sectional areas $A_a = h_a w_a$, $A_b = h_b w_b$ and $A_c = h_c w_c$. The total cross-sectional area is $A = 2A_a + 2A_b + A_c$.

The material of the piezoelectric layers is assumed to be elastic with closed-circuit Young's modulus E_a, while the materials of the bonding layers and the core are assumed to be viscoelastic with complex modules $E_b(\omega)$ and $E_c(\omega)$. As special cases, one or both of the latter materials may be considered elastic by taking their complex modules as real-valued and constant. It is assumed that initially plane cross-sections remain plane and that the stress is uniaxial in the x direction. Therefore, the effective complex modulus of the PBE is $E = (2A_aE_a + 2A_bE_b + A_cE_c)/A$. Similarly, the effective density of the PBE is $\rho = (2A_a\rho_a + 2A_b\rho_b + A_c\rho_c)/A$, where ρ_a, ρ_b and ρ_c are the densities of the piezoelectric, bonding and core layers, respectively.

The piezoelectric material is assumed to be polarized in the z direction and to have linear electromechanical response. In addition to the closed-circuit Young's modulus E_a, this response is characterized by the permittivity ε_a and the piezoelectric constant d_a (commonly denoted $-d_{31}$). The electrical fields between the electrodes on the upper and lower faces of the actuators are assumed to be parallel to the z-axis. The electric displacement field is assumed to depend on x and ω, while the electric field strength is assumed to depend on ω only. The electrodes of the piezoelectric layers are assumed to be connected in parallel in such a way that these layers deform in phase when a voltage is supplied to the electrical port. The effects of strains in the transverse directions are neglected.

In Appendix A it is shown that the four independent impedance elements of the laminated PBE are

$$Z_{00} = \frac{1}{2}\frac{Z^E_a}{1-k^2_a}, \quad Z_{01} = \frac{d_a h_a}{\varepsilon_a A_a}\frac{Z^M_a}{1-k^2_a} = A_a E_a \frac{d_a}{h_a}\frac{Z^E_a}{1-k^2_a}, \tag{4a,b}$$

$$Z_{11} = 2\frac{k^2_a Z^M_a}{1-k^2_a} + \frac{Z^M_{ch}}{\tanh(\gamma l)}, \quad Z_{12} = 2\frac{k^2_a Z^M_a}{1-k^2_a} + \frac{Z^M_{ch}}{\sinh(\gamma l)}. \tag{4c,d}$$

Here $Z^E_a = 1/\mathrm{i}\omega C_a$ is the electrical impedance of a single mechanically unloaded piezoelectric layer with capacitance $C_a = \varepsilon_a w_a l/h_a$, $Z^M_a = K_a/\mathrm{i}\omega$ is the quasi-static mechanical impedance of a single electrically short-circuited piezoelectric layer with stiffness $K_a = A_a E_a/l$, and $k^2_a = d^2_a E_a/\varepsilon_a$ is the electromechanical coupling coefficient. Furthermore, $Z^M_{\mathrm{ch}} = AE/c$ is the characteristic impedance, $c = (E/\rho)^{1/2}$ is the wave speed and $\gamma = \mathrm{i}\omega/c$ is the wave propagation coefficient. Through the definition of these parameters and of the cross-sectional area A, the effective complex modulus E and the effective density ρ, the four impedance elements that

define the impedance matrix are expressed in terms of 15 basic parameters out of which eight are related to the materials (E_a, ρ_a, ε_a, d_a; E_b, ρ_b; E_c, ρ_c) and seven to the geometry (h_a, w_a, h_b, w_b, h_c, w_c, l) of the PBE.

If the layers b and c are elastic, then E, c and Z^M_{ch} are real and therefore the impedance elements given by Eq. (4) are imaginary. This implies that the impedance matrix is imaginary and confirms that such a laminated PBE is free from losses.

In the absence of piezoelectricity $d_a = 0$ and $k_a = 0$, and therefore the impedance elements Z_{ij} of Eq. (4) are reduced to

$$Z'_{00} = \frac{1}{2}Z^E_a, \quad Z'_{01} = 0, \quad Z'_{11} = \frac{Z^M_{\text{ch}}}{\tanh(\gamma l)}, \quad Z'_{12} = \frac{Z^M_{\text{ch}}}{\sinh(\gamma l)}. \tag{5a–d}$$

In Eqs. (4) and (5), the terms $Z^M_{\text{ch}}/\tanh(\gamma l)$ and $Z^M_{\text{ch}}/\sinh(\gamma l)$ determine whether the response of the PBE is dynamic or quasi-static. At angular frequencies $\omega \ll |c|/l$, both terms approach $K/\mathrm{i}\omega$, where $K = AE/l$ is the stiffness of the PBE, and the response of the PBE is quasi-static. At such low frequencies, and in the absence of piezoelectricity, the last two of Eq. (1) become $\hat{N}_1 = \hat{N}_2 = K(\hat{u}_2 - \hat{u}_1)$, where $\hat{u}_1 = \hat{v}_1/\mathrm{i}\omega$ and $\hat{u}_2 = \hat{v}_2/\mathrm{i}\omega$ are displacements corresponding to the velocities $\hat{v}_1$ and $\hat{v}_2$.

3. Generation of extensional waves

3.1. Current and waves

Let the PBE constitute a part of a long bar, elastic or viscoelastic, and consider how extensional waves are generated when the PBE is driven with an input voltage $\hat{U}_0$. The external parts of the bar are assumed to be semi-infinite and to have equal characteristic impedances $Z_1(\omega) = Z_2(\omega)$ as shown in Fig. 2(a). The driving voltage produces a current $\hat{i}_0$ and generates extensional waves, which propagate away from the PBE in opposite directions. Because of the symmetry, these waves are associated with the same normal force $\hat{N}_G(\omega)$ at the two mechanical interfaces. In the absence of waves propagating towards the PBE, this force is related to the interface forces and velocities by the continuity conditions

$$\hat{N}_1 = \hat{N}_G, \quad \hat{v}_1 = \frac{1}{Z_1}\hat{N}_G, \tag{6a,b}$$

$$\hat{N}_2 = \hat{N}_G, \quad \hat{v}_2 = -\frac{1}{Z_2}\hat{N}_G. \tag{6c,d}$$

As $\hat{N}_2 = \hat{N}_1$ and $\hat{v}_2 = -\hat{v}_1$, the last two of the three scalar equations (1) are the same. Therefore, Eqs. (1) and (6) provide six independent equations for the six unknowns $\hat{i}_0, \hat{v}_1, \hat{v}_2, \hat{N}_1, \hat{N}_2$ and $\hat{N}_G$. Solving for $\hat{i}_0$ and $\hat{N}_G$, one obtains

$$\hat{i}_0 = \frac{Z_{11} + Z_{12} + Z_1}{Z_{00}(Z_{11} + Z_{12} + Z_1) - 2Z^2_{01}}\hat{U}_0, \tag{7}$$

$$\hat{N}_G = \frac{Z_{01}Z_1}{Z_{00}(Z_{11} + Z_{12} + Z_1) - 2Z^2_{01}}\hat{U}_0. \tag{8}$$

The internal (input) impedance is $Z^E_{\text{int}} = \hat{U}_0/\hat{i}_0$, i.e.,

$$Z^E_{\text{int}} = Z_{00} - \frac{2Z^2_{01}}{Z_{11} + Z_{12} + Z_1}. \tag{9}$$

It depends on the four impedances characterizing the PBE and on the characteristic impedance of the external parts of the bar. The equivalent electrical circuit is shown in Fig. 2(b).

3.2. Energy

Temporarily, let the assembly consist of a lossless PBE with imaginary impedance matrix, $Z_{ij} = \mathrm{i}X_{ij}$, and an elastic bar with real characteristic impedance $Z_1 = R_1$. An example of such a PBE is the laminated one in Fig. 1(b) with its bonding and core layers b and c elastic. Let also the input voltage to the PBE be harmonic and again interpret Fourier transforms as complex effective amplitudes. Then the electrical average power

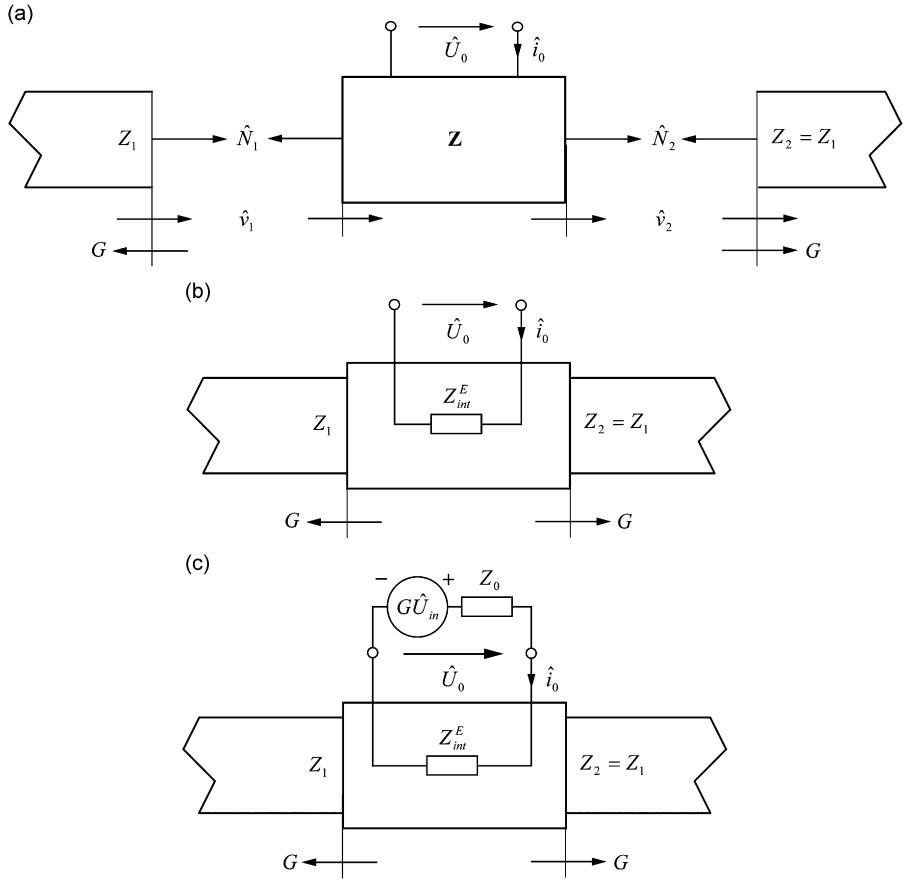

Fig. 2. Generation of extensional waves in a long viscoelastic or elastic bar. Propagation directions of generated (G) waves indicated by arrows. (a) Interaction of PBE and bar at mechanical interfaces. Equivalent electrical circuit for PBE driven by (b) input voltage $\hat{U}_0$ and (c) linear amplifier with input voltage $\hat{U}_{\text{in}}$, voltage gain G unloaded and output impedance Z_0.

supplied to the assembly is $P_0 = \text{Re}(Z^E_{\text{int}})\left|\hat{i}_0\right|^2$ and the average energy flux of each of the two waves generated in the bar is $P_G = (1/R_1)\left|\hat{N}_G\right|^2$. Therefore, the ratio $p_G = P_G/P_0$ can be determined by substituting Eqs. (7)–(9) with $Z_1 = R_1$ and $Z_{ij} = \text{i}X_{ij}$. The result is $p_G = 1/2$ or

$$P_G = \frac{1}{2}P_0, \tag{10}$$

which confirms that energy is conserved.

3.3. Input from linear power amplifier

Fig. 2(c) shows the equivalent electrical circuit when the driving voltage $\hat{U}_0$ is supplied by a linear power amplifier with input voltage $\hat{U}_{\text{in}}(\omega)$, with gain $G(\omega)$ unloaded and with output impedance $Z_0(\omega)$. Here the driving voltage can be expressed in terms of the input voltage to the amplifier as

$$\hat{U}_0 = \frac{Z^E_{\text{int}}}{Z^E_{\text{int}} + Z_0} G\hat{U}_{\text{in}}. \tag{11}$$

This expression shows that the voltage gain G of the unloaded amplifier is modified by the factor $Z^E_{\text{int}}/(Z^E_{\text{int}} + Z_0)$ when the amplifier is loaded by the internal (input) impedance Z^E_{int} of the PBE. In the special case $Z_0/Z^E_{\text{int}} = 0$, Eq. (11) becomes $\hat{U}_0 = G\hat{U}_{\text{in}}$.

Substituting Eq. (11) into Eqs. (7) and (8), one can express the current $\hat{i}_0$ driven into the PBE and the waves $\hat{N}_G$ generated in the bar in terms of the input voltage $\hat{U}_{\text{in}}$ to the amplifier. Specializing to the laminated PBE by introducing also the impedance elements (4), one obtains expressions for, e.g., $\hat{N}_G$ and Z^E_{int} that agree with those of Ref. [14].

3.4. Other cases

Results for other cases of mechanical environment can be obtained from Eqs. (6)–(9) by considering extreme limits of the characteristic impedance Z_1 of the bars, by replacing Z_1 by impedances of other mechanical devices and by considering symmetry. The first two ways lead to results for new symmetric systems, while the third way gives results for new asymmetric systems.

Results for a PBE sandwiched between rigid walls is obtained in the limit $Z_1 \to \infty$. For such a system, the internal impedance is $Z^E_{\text{int}} = Z_{00}$. Similarly, results for a PBE free at both of its mechanical interfaces is obtained for $Z_1 = 0$. For such a system, the internal impedance is $Z^E_{\text{int}} = Z_{00} - 2Z^2_{01}/(Z_{11} + Z_{12})$.

Consider next a case where the two semi-infinite bars are replaced by finite bars, free at their outer ends and with length l_1, wave speed c_1 and characteristic impedance Z_1. Then, instead of Z_1, the impedance faced by the PBE at each mechanical port is $Z_1 \tanh(\gamma_1 l_1)$ with $\gamma_1 = \mathrm{i}\omega/c_1$. Therefore, the forces and velocities at the mechanical interfaces, the current at the electrical interface and the internal impedance can be obtained by replacing Z_1 by $Z_1 \tanh(\gamma_1 l_1)$ in the corresponding results for the semi-infinite bars. However, it should be noted that here $\hat{N}_G$ does not represent outgoing waves.

Because of the assumed symmetry, the particle velocity is zero at the mid-plane $x = 0$ of the PBE. Furthermore, no current can pass through this plane. Therefore, results can be obtained for, say, the right half of each of the above systems with a rigid non-conducting wall on its left side. In these cases, the current given by Eq. (7) is halved and correspondingly the internal impedance given by Eq. (9) is doubled. In the absence of piezoelectricity, $Z^E_{\text{int}} = Z'_{00}$ in the symmetrical cases and $Z^E_{\text{int}} = 2Z'_{00}$ in the asymmetrical cases.

4. Damping of extensional waves

4.1. Voltage, current and waves

Let again the PBE constitute a part of a long viscoelastic bar with characteristic impedance $Z_1(\omega) = Z_2(\omega)$, but now let the electrical port be shunted by an external impedance load $Z_0(\omega)$ as shown in Fig. 3(a). Also, let an incident wave propagating towards the PBE be represented by the normal force $\hat{N}_I(\omega)$ at the first mechanical interface, and consider the generation of a voltage $\hat{U}_0$ and a current $-\hat{i}_0$ at the electric port, and reflected and transmitted waves $\hat{N}_R(\omega)$ and $\hat{N}_T(\omega)$ at the first and second mechanical interfaces, respectively. The forces associated with the three waves are related to the interface forces and velocities by the continuity conditions

$$\hat{N}_1 = \hat{N}_I + \hat{N}_R, \quad \hat{v}_1 = \frac{1}{Z_1}(-\hat{N}_I + \hat{N}_R), \tag{12a,b}$$

$$\hat{N}_2 = \hat{N}_T, \quad \hat{v}_2 = -\frac{1}{Z_2}\hat{N}_T. \tag{12c,d}$$

The voltage and current at the electrical port are related by

$$\hat{U}_0 = Z_0(-\hat{i}_0). \tag{12e}$$

Here, Eqs. (1) and (12) provide eight independent equations for the eight unknowns $\hat{i}_0, \hat{v}_1, \hat{v}_2, \hat{U}_0, \hat{N}_1, \hat{N}_2, \hat{N}_R$ and $\hat{N}_T$. Solving first for $\hat{U}_0$ and $-\hat{i}_0$, one obtains

$$\hat{U}_0 = \frac{2Z_{01}Z_0}{(Z_{11} + Z_{12} + Z_1)(Z_{00} + Z_0) - 2Z^2_{01}}\hat{N}_I, \tag{13a}$$

$$-\hat{i}_0 = \frac{2Z_{01}}{(Z_{11} + Z_{12} + Z_1)(Z_{00} + Z_0) - 2Z^2_{01}}\hat{N}_I. \tag{13b}$$

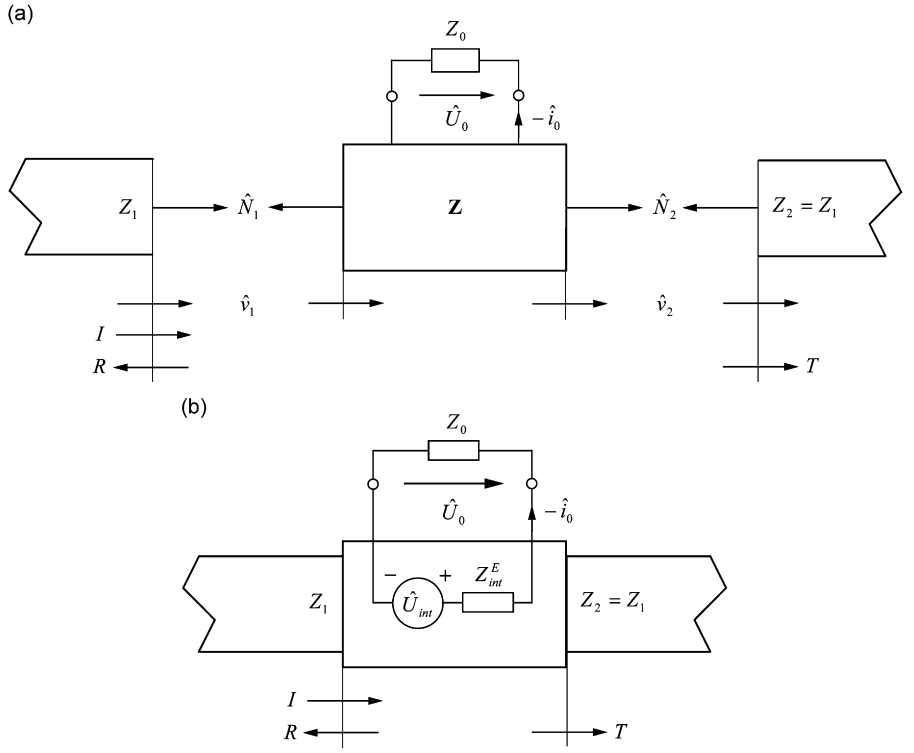

Fig. 3. Damping of extensional waves in a long viscoelastic or elastic bar. Propagation directions of incident (I), reflected (R) and transmitted (T) waves indicated by arrows. (a) Interaction of PBE and bar at mechanical interfaces. (b) Equivalent electrical circuit for PBE feeding shunted impedance load Z_0.

The first of these equations can be rewritten as

$$\hat{U}_0 = \frac{Z_0}{Z_{\text{int}}^E + Z_0}\hat{U}_{\text{int}}, \quad \hat{U}_{\text{int}} = \frac{2Z_{01}}{Z_{11} + Z_{12} + Z_1}\hat{N}_I, \tag{14a,b}$$

where $Z_{\text{int}}^E(\omega)$ is the internal (output) impedance given by Eq. (9) and $\hat{U}_{\text{int}}(\omega)$ is the internal voltage generated by the incident wave. The equivalent electrical circuit is shown in Fig. 3(b). Solving also for $\hat{N}_R$ and $\hat{N}_T$, one obtains

$$\hat{N}_R = \frac{(Z_{11}^2 - Z_{12}^2 - Z_1^2)(Z_{00} + Z_0) - 2Z_{01}^2(Z_{11} - Z_{12})}{((Z_{11} + Z_1)^2 - Z_{12}^2)(Z_{00} + Z_0) - 2Z_{01}^2(Z_{11} - Z_{12} + Z_1)}\hat{N}_I, \tag{15a}$$

$$\hat{N}_T = \frac{2Z_1(Z_{12}(Z_{00} + Z_0) - Z_{01}^2)}{((Z_{11} + Z_1)^2 - Z_{12}^2)(Z_{00} + Z_0) - 2Z_{01}^2(Z_{11} - Z_{12} + Z_1)}\hat{N}_I. \tag{15b}$$

In the absence of piezoelectricity $Z_{ij} = Z'_{ij}$ and $Z'_{01} = 0$, and these relations become

$$\hat{N}_R = \frac{Z'^2_{11} - Z'^2_{12} - Z_1^2}{(Z'_{11} + Z_1)^2 - Z'^2_{12}}\hat{N}_I, \quad \hat{N}_T = \frac{2Z_1 Z'_{12}}{(Z'_{11} + Z_1)^2 - Z'^2_{12}}\hat{N}_I. \tag{16a,b}$$

4.2. Energy

The energy delivered to the external load Z_0 at time t is

$$W_0 = \int_0^t U_0(-i_0)\,\mathrm{d}\tau, \tag{17}$$

and the energies associated with the complete incident, reflected and transmitted waves are

$$W_I = \frac{1}{Z_1}\int_0^\infty N_I^2(t)\,\mathrm{d}t, \quad W_R = \frac{1}{Z_1}\int_0^\infty N_R^2(t)\,\mathrm{d}t, \quad W_T = \frac{1}{Z_1}\int_0^\infty N_T^2(t)\,\mathrm{d}t, \tag{18a–c}$$

respectively. The energy dissipated in the external load after a long time is $W_D = W_0(\infty)$, and the relative energy dissipation is defined as

$$w_D = \frac{W_D}{W_I}. \tag{19}$$

Temporarily, again, let the assembly consist of a lossless PBE with imaginary impedance matrix, $Z_{ij} = \mathrm{i}X_{ij}$, and an elastic bar with real characteristic impedance $Z_1 = R_1$. Let also the incident wave be harmonic and interpret again Fourier transforms as complex effective amplitudes. Furthermore, let the impedance of the external load $Z_0 = R_0 + \mathrm{i}X_0$ be chosen as the complex conjugate of the internal impedance Z_{int}^E in order to maximize the supply of electrical power to the load, i.e., $Z_0 = \bar{Z}_{\mathrm{int}}^E$. Then, the average energy flux of the incident wave is $P_I = (1/R_1)\left|\hat{N}_I\right|^2$, and those of the reflected and transmitted waves are $P_R = (1/R_1)\left|\hat{N}_R\right|^2$ and $P_T = (1/R_1)\left|\hat{N}_T\right|^2$, respectively. Due to the impedance matching, the electrical average power dissipated in the load can be expressed as $P_D = (1/R_0)\left|\hat{U}_{\mathrm{int}}/2\right|^2$. Therefore, the ratios $p_R = P_R/P_I$, $p_T = P_T/P_I$ and $p_D = P_D/P_I$ can be determined by substituting Eqs. (9), (14b) and (15) with $Z_1 = R_1$, $Z_{ij} = \mathrm{i}X_{ij}$ and $R_0 = \mathrm{Re}(Z_{\mathrm{int}}^E)$. The result is $p_R = p_T = \frac{1}{4}$ and $p_D = \frac{1}{2}$. Therefore

$$P_R = P_T = \tfrac{1}{4}P_I, \quad P_D = \tfrac{1}{2}P_I, \tag{20a,b}$$

which confirms that energy is conserved. Under the conditions assumed, the reflected and transmitted waves turn out to have equal magnitudes and opposite phases,

$$-\hat{N}_R = \hat{N}_T = \frac{1}{2}\frac{R_1 - \mathrm{i}(X_{11} - X_{12})}{R_1 + \mathrm{i}(X_{11} - X_{12})}\hat{N}_I. \tag{21}$$

4.3. Two-port representation

The PBE with the electrical port shunted can also be given a two-port representation similar to that given by Eq. (3b) in the absence of piezoelectricity. By eliminating $\hat{U}_0$ and $\hat{i}_0$ from the four equations (1) and (12e), one obtains

$$\begin{bmatrix} \hat{N}_1 \\ \hat{N}_2 \end{bmatrix} = \begin{bmatrix} Z''_{11} & Z''_{12} \\ Z''_{21} & Z''_{22} \end{bmatrix} \begin{bmatrix} -\hat{v}_1 \\ \hat{v}_2 \end{bmatrix}, \tag{22}$$

where

$$Z''_{ij} = Z_{ij} - \frac{Z_{01}^2}{Z_{00} + Z_0}. \tag{23}$$

Some special cases of interest are (i) closed terminals, $Z_0 = 0$ and $Z''_{ij} = Z_{ij} - Z_{01}^2/Z_{00}$; (ii) open terminals, $Z_0 \to \infty$ and $Z''_{ij} \to Z_{ij}$; and (iii) absence of piezoelectricity, $d_a = 0$ and $Z''_{ij} = Z'_{ij}$.

4.4. Numerical results

Results of numerical simulations will be presented for damping of waves by use of a laminated PBE of the type described in Section 2.2. The geometrical and material parameters will be those of the laminated PBE used in the experimental wave generation tests of Ref. [15]. Thus, a long aluminium bar with square cross-section $4.0 \times 4.0\,\mathrm{mm}^2$ is considered. Over a length of $l = 95.4\,\mathrm{mm}$, the height of the bar is reduced symmetrically to $h_c = 1.02\,\mathrm{mm}$, while the width $w_c = 4.0\,\mathrm{mm}$ is the same as in the rest of the bar. This part of the bar constitutes the core c of the laminated PBE. The Young's modulus and density of aluminium are taken

as $E_c = 69\,\text{GPa}$ and $\rho_c = 2\,700\,\text{kg/m}^3$, respectively. Two piezoelectric elements with height $h_a = 0.66\,\text{mm}$ and width $w_a = 6.4\,\text{mm}$ are bonded to the upper and lower surfaces of the core, symmetrically and along the full length of the core. They constitute the layers a of the laminated PBE. The piezoelectric material of ceramic type is characterized by closed-circuit Young's modulus $E_a = 66\,\text{GPa}$, density $7\,800\,\text{kg/m}^3$, piezoelectric constant $d_a = 190 \times 10^{-12}\,\text{m/V}$ and permittivity $\varepsilon_a = 1.6 \times 10^{-8}\,\text{As/Vm}$. The bonding layers b are assumed to be thin enough to be neglected.

These dimensions and material properties correspond to parameters as follows. The wave speed is $c = 3300\,\text{m/s}$ in the PBE and 5050 m/s in the external parts of the bar. The transit time for a wave through the PBE is $t_{\text{tr}} = l/c = 28.9\,\mu\text{s}$. The characteristic impedance of the PBE is $Z_{\text{ch}}^M = 254\,\text{Ns/m}$ and that of the external parts of the bar is $Z_1 = Z_2 = 219\,\text{N s/m}$. The capacitance of a single mechanically unloaded piezoelectric element is $C_a = 14.7\,\text{nF}$, and the electromechanical coupling coefficient is $k_a{}^2 = 0.150$. At frequencies approaching zero, the real part $R_{\text{int}}^E(\omega)$ of the internal impedance $Z_{\text{int}}^E(\omega)$ of the PBE approaches the limit $R_{\text{int}}^{\text{DC}}(\omega) = 46.4\,\Omega$.

The electrical load is taken as a serial RL circuit with resistance R_0 and inductance L_0. The load impedance $Z_0 = R_0 + \text{i}\omega L_0$ is expressed as

$$Z_0 = R_0(1 + \text{i}\omega t_0), \tag{24}$$

where $t_0 = L_0/R_0$ is a characteristic time. The incident wave is defined by the bell-shaped pulse

$$N_I = \widehat{N}_I \sin^2(\pi t/t_I)[\theta(t) - \theta(t - t_I)], \tag{25}$$

where $\widehat{N}_I$ is the amplitude, t_I is the duration and $\theta(t)$ is the Heaviside unit step function.

Simulations were carried out for $R_0/R_{\text{int}}^{\text{DC}} = 0.2, 1, 5$ and 20, $t_0/t_{\text{tr}} = 0.05,\ 0.1,\ 0.2,\ 0.5,\ \ldots,\ 100$ and $t_I/t_{\text{tr}} \in (0.1,\ 10)$. The amplitude of the incident wave was set to $\widehat{N}_I = 10\,\text{N}$. Because of the linearity of the system, this value is immaterial from a theoretical point of view. However, it is considered to be realistic in experimental implementations.

The frequency dependence of the internal impedance Z_{int}^E and the load impedance Z_0 with $R_0 = R_{\text{int}}^{\text{DC}}$ and $t_0 = t_{\text{tr}}$ is shown in Fig. 4, while Fig. 5 shows the time dependence of the normal forces N_I associated with incident waves of durations $t_I = 0.5t_{\text{tr}}$, t_{tr} and $2t_{\text{tr}}$, and the corresponding spectra. For the load of Fig. 4 and the incident waves of Fig. 5, Fig. 6 shows the time dependence of the normal forces N_R and N_T associated with the reflected and transmitted waves. Similarly, Fig. 7 shows the time dependence of the voltage U_0 generated across the load, the current $-i_0$ driven into the load, and the power P_0 and the energy W_0 supplied to the load. The dependence of the relative energy dissipation $w_D = W_D/W_I$ on the normalized duration t_I/t_{tr} of the incident wave for different normalized resistances $R_0/R_{\text{int}}^{\text{DC}}$ and characteristic times t_0/t_{tr} of the load is shown in Fig. 8.

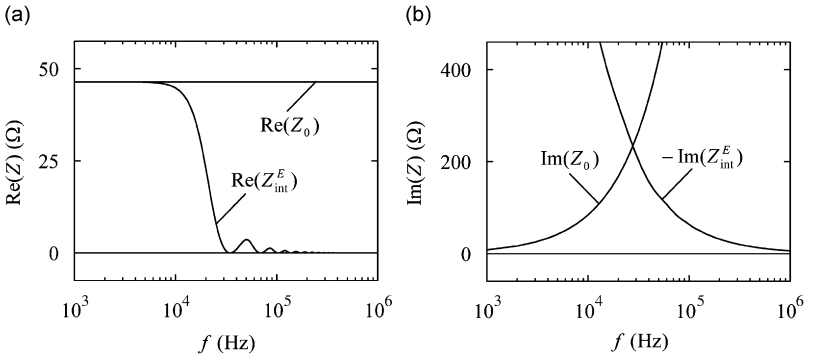

Fig. 4. Internal impedance Z_{int}^E and load impedance Z_0 versus frequency f for $R_0 = R_{\text{int}}^{\text{DC}}$ and $t_0 = t_{\text{tr}}$: (a) real parts and (b) imaginary parts.

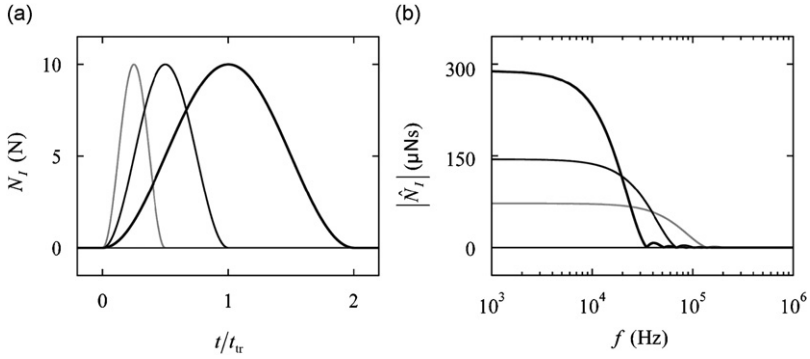

Fig. 5. (a) Normal forces N_I associated with incident waves versus time t and (b) corresponding spectra $|\hat{N}_I|$ versus frequency f. Incident wave with duration $t_I = 0.5t_{tr}$ (grey curves), t_{tr} (thin curves) and $2t_{tr}$ (thick curves).

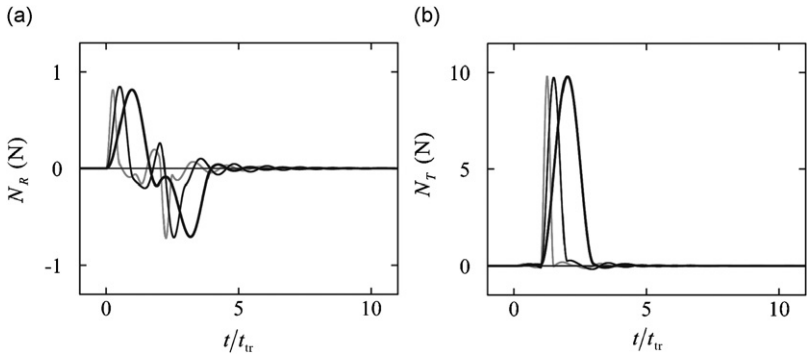

Fig. 6. Normal forces (a) N_R associated with reflected waves and (b) N_T associated with transmitted waves versus time t for $R_0 = R_{int}^{DC}$ and $t_0 = t_{tr}$. Incident wave with duration $t_I = 0.5t_{tr}$ (grey curves), t_{tr} (thin curves) and $2t_{tr}$ (thick curves).

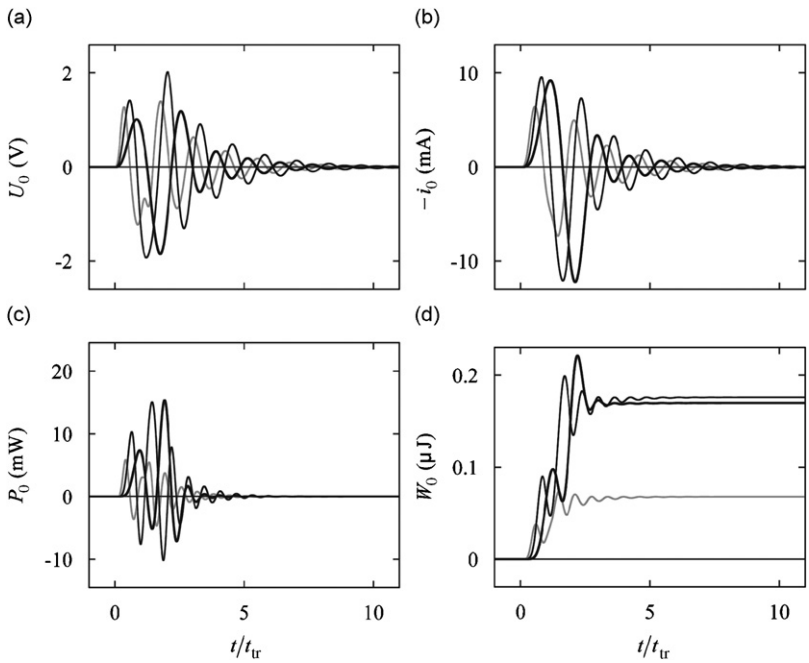

Fig. 7. (a) Voltage U_0 generated across the load, (b) current $-i_0$ driven into the load, (c) power P_0 supplied to the load and (d) energy W_0 supplied to the load versus time t for $R_0 = R_{int}^{DC}$ and $t_0 = t_{tr}$. Incident wave with duration $t_I = 0.5t_{tr}$ (grey curves), t_{tr} (thin curves) and $2t_{tr}$ (thick curves).

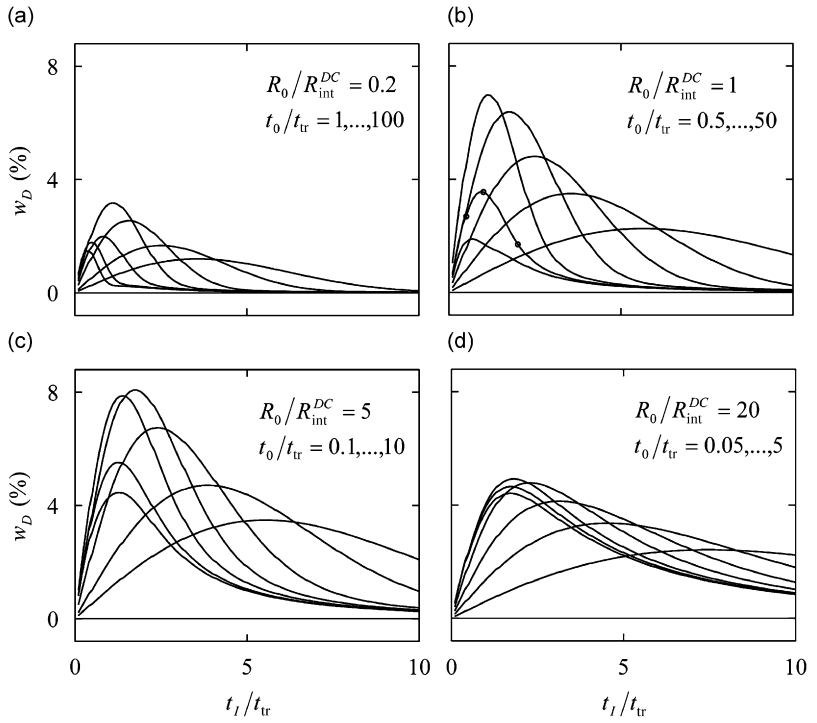

Fig. 8. Relative dissipation $w_D = W_D/W_I$ versus normalized duration t_I/t_{tr} of incident wave for different normalized resistances $R_0/R_{\text{int}}^{\text{DC}}$ and characteristic times t_0/t_{tr} of the load. The maxima move from left to right with increasing t_0/t_{tr}: (a) $R_0/R_{\text{int}}^{\text{DC}} = 0.2$ and $t_0/t_{\text{tr}} = 1, 2, 5, \ldots, 100$; (b) $R_0/R_{\text{int}}^{\text{DC}} = 1$ and $t_0/t_{\text{tr}} = 0.5, 1, 2, \ldots, 50$; (c) $R_0/R_{\text{int}}^{\text{DC}} = 5$ and $t_0/t_{\text{tr}} = 0.1, 0.2, 0.5, \ldots, 10$ and (d) $R_0/R_{\text{int}}^{\text{DC}} = 20$ and $t_0 = t_{\text{tr}} = 0.05, 0.1, 0.2, \ldots, 5$.

5. Discussion

A straight bar element containing axially oriented piezoelectric members, referred to as the PBE, has been viewed as a linear system with one electrical and two mechanical interfaces or ports. Its interactions with external devices have been described in terms of voltage and current at the electrical port and force and velocity at the mechanical ports. As far as these interactions are concerned, and due to symmetry and reciprocity assumed, it has been shown that the properties of the PBE are defined by four elements of a 3×3 impedance matrix. These elements have been derived for a specific laminated PBE, previously studied theoretically [14] and experimentally [15]. The three-port model of the PBE has been applied to generation and damping of extensional waves in a long bar.

The principal advantages of the three-port approach stem from the fact that the dynamics and characteristics of the PBE are independent of external devices as well as of its use as actuator or sensor. The dynamics is represented by the three scalar equation (1) for any PBE considered, while the characteristics of a specific PBE are defined by the specific expressions for the four elements of the impedance matrix. On the one hand, therefore, results for different environments or uses can be derived without specifying the PBE. For the mechanical environment of an elastic or viscoelastic bar, this has been illustrated by the examples of generation and damping of extensional waves. In these examples, the PBE is used as an actuator driven by a linear power amplifier and as a sensor shunted by an electrical impedance, respectively. On the other hand, the characteristics of a specific PBE can be derived without reference to its environment or use. This has been illustrated by the derivation of the impedance elements of a specific laminated PBE.

When results are to be derived for a certain environment and use of a general PBE, a few equations representing the external devices must be added to the three scalar equations (1). This has been illustrated in the examples of generation and damping of extensional waves. Thus, for the mechanical environment of an elastic or viscoelastic bar, the five equations (6) and (11) were added in the first and the five equations (12) in

the second of these examples. The addition of equations results in linear systems of equations that can be solved for voltage, current, forces and velocities. From the solutions for voltage and current, the internal impedance of the PBE can be determined. It should be noted that the derivation of the four impedance elements, constituting coefficients in some of the equations, is much more involved than the solution of the linear system of equations. It generally requires, e.g., the solution of partial differential equations, which is a good reason for treating the two problems separately.

One case of a specific PBE has been considered as an example, viz., the laminated one shown in Fig. 1(b) with one pair of piezoelectric layers, one pair of bonding layers and one core, all with the full length of the PBE. Other cases covered by the three-port model may have additional piezoelectric, elastic or viscoelastic pairs of layers, and these pairs may have different lengths. Also, the constitutive properties may be different for the materials of different pairs of piezoelectric layers. In this way, the geometrical and material properties of the cross-sections may vary in the axial direction. On the basis of assumptions of plane cross-sections and one-dimensional wave propagation, it is feasible to determine the impedance elements for such complex PBEs even though the analyses may get much more involved than in the example.

The assumption that initially plane cross-sections remain plane means that the effect of shear deformation of the bonding layers is neglected. This can be justified if the bonding layers are very thin, or the bonding material is very stiff, or both. It should be noted that the effects of axial stiffness and inertia, taken into account here for the laminated PBE, may be significant even if that of shear deformation is not. This is the case if the modulus and density of the bonding layers are high enough. The use of one-dimensional analysis implies that the significant wavelengths must be large relative to the transverse dimensions. In experimental studies [15] with a laminated PBE of the same type as in the example, good agreement was obtained between experimental and theoretical results when one-dimensional analysis was used and all effects of the bonding layers were neglected.

The consistency of the models used has been confirmed by considering balances of electrical power and energy fluxes associated with harmonic waves for a lossless PBE and an elastic bar. First, it has been shown that such a PBE corresponds to an impedance matrix with imaginary elements. Then, for the process of wave generation it has been shown that the electrical input power is partitioned equally between the energy fluxes associated with the two harmonic waves generated in the bar. In the equivalent electrical circuit of Fig. 2(b), the dissipation of power associated with the resistive part of the internal impedance Z^E_{int} corresponds to the sum of these energy fluxes. In analogy with the terminology used for dipole antennas, this resistive part might be referred to as the radiation resistance [18] of the PBE-bar assembly. Similarly, for the process of wave damping, and under the additional condition of electrical impedance matching, it has been shown that half of the mechanical input power is dissipated in the impedance load, and one quarter of it is made up of the energy fluxes associated with each of the reflected and transmitted waves. In the equivalent electrical circuit of Fig. 3(b), the dissipation of power in the resistive part of the internal impedance Z^E_{int} corresponds to the sum of these energy fluxes.

It may appear surprising that in the process of wave damping the partition of power is independent of all other conditions than the ones mentioned. In particular, it may seem strange that the power $P_D = (1/R_0)\left|\hat{U}_{\text{int}}/2\right|^2$ dissipated in the resistive part R_0 of the load remains the same even in the limit of vanishing piezoelectricity, i.e., $d_a \to 0$, which implies $Z_{01} = \mathrm{i}X_{01} \to 0$. However, the explanation is given by the condition for impedance matching, $Z_0 = \overline{Z}^E_{\text{int}}$. Due to the assumed fulfillment of this condition, the resistive part of the load is $R_0 \propto X^2_{01}$, and the voltage across this part of the load is $\left|\hat{U}_{\text{int}}/2\right| \propto X_{01}$. Therefore, the dissipated power does not depend on X_{01}. In practice, the validity of this independence is limited as the resistive part of the load cannot be arbitrarily small.

Comparison of Figs. 4 and 5 gives an idea about the degree of mismatch of the load impedance $Z_0 = R_0(1 + \mathrm{i}\omega t_0)$ to the internal impedance Z^E_{int} at frequencies of importance for the wave damping results shown in Figs. 6 and 7. Fig. 4 shows that when $R_0 = R^{\text{DC}}_{\text{int}}$ and $t_0 = t_{\text{tr}}$, the matching condition $Z_0 = \overline{Z}^E_{\text{int}}$ for maximum delivery of electrical power to the load is not fulfilled at any frequency. This is normal as the real and imaginary parts of this condition cannot in general be satisfied at the same frequency. Here, the real part $\text{Re}(Z_0) = \text{Re}(Z^E_{\text{int}})$ is approximately fulfilled below 7 kHz and the imaginary part $\text{Im}(Z_0) = -\text{Im}(Z^E_{\text{int}})$ is satisfied only at the resonance frequency 27.8 kHz. In Fig. 5, these observations can be compared with the spectra for the three incident waves N_I used as input for the results shown in Figs. 6 and 7. These waves have

durations $t_I = 0.5t_{tr}$, t_{tr} and $2t_{tr}$, and the important frequency ranges of their spectra are from DC up to about 100, 50 and 25 kHz, respectively. The PBE and bar defined for the simulations have wave speeds 3300 and 5050 m/s. Therefore, the highest frequency of importance, 100 kHz, corresponds to wavelengths of 33 and 51 mm, respectively, which are much longer than the transverse dimensions of about 4 mm.

As shown by Fig. 6, the initial main part of the reflected wave N_R is first positive and then negative, while that of the transmitted wave N_T is essentially positive and resembles the incident wave. Both waves are followed by damped oscillating tails. These tails are explained by repeated wave reflections within the PBE due to the mechanical mismatch between the PBE, with characteristic impedance $Z_{ch}^M = 254\,\mathrm{N\,s/m}$, and the external parts of the bar, with characteristic impedance $Z_1 = Z_2 = 219\,\mathrm{N\,s/m}$. The reflected wave starts at the time $t = 0$ when the front of the incident wave arrives at the first mechanical interface. The main rise of the transmitted wave at the second mechanical interface occurs at $t = t_{tr}$, after one transit time through the PBE. However, a slow rise of the transmitted wave starts already at $t = 0$. This is because the electric field has been assumed to be a function of time only, corresponding to infinite speed of electromagnetic waves.

As shown by Fig. 7, the voltage U_0 generated across the load, the current $-i_0$ driven into the load and the power P_0 supplied to the load are all oscillatory. The oscillations are first built up and then they form tails, which rapidly decay. The energy W_0 supplied to the load increases, while oscillating, up to the final level W_D representing the energy dissipated in the resistive part of the load. The amplitude of the current $-i_0$ produced by the shortest incident wave ($t_I = 0.5t_{tr}$) is considerably lower than that produced by the two longer waves ($t_I = t_{tr}$ and $2t_{tr}$), which are similar. Correspondingly, the dissipated energy $W_D = R_0 \int_0^\infty i_0^2\,\mathrm{d}t$ due to the shortest incident wave is considerably lower than those produced by the two longer waves, which are similar. In particular, the energy dissipated due to the shortest incident wave is less than half of that produced by the middle wave.

The observations made imply that the relative energy dissipation $w_D = W_D/W_I$ is lower for the shortest and longest incident waves than for the middle wave. For the shortest incident wave it is lower because relative to the middle wave, W_I is smaller by a factor two while W_D is smaller by a factor larger than two. For the longest incident wave, it is lower because relative to the middle wave, W_I is larger by a factor two while W_D is approximately equal. The three cases of incident waves discussed so far are marked with circles in Fig. 8, which for different normalized load parameters R_0/R_{int}^{DC} and t_0/t_{tr} show how the relative energy dissipation $w_D = W_I/W_D$ depends on the normalized duration t_I/t_{tr} of the incident wave. For the shortest, the middle and the longest incident waves the relative dissipation turns out to be $w_D = 2.7\%$, 3.6% and 1.7%, respectively.

For given load parameters R_0/R_{int}^{DC} and t_0/t_{tr}, corresponding to one of the curves shown in the four diagrams of Fig. 8, w_D has a maximum for a certain duration t_I/t_{tr} of the incident wave and approaches zero for both short and long durations. When the time constant t_0/t_{tr} of the load increases from small to large, as it does by two decades in each diagram, the maxima with respect to t_I/t_{tr} move from left to right. On the way, w_D first increases to a largest value and then decreases. When, finally, the resistive part R_0/R_{int}^{DC} of the load increases from small to large, as it does by one decade from the first diagram to the last, the maxima with respect to t_I/t_{tr} and t_0/t_{tr} increase to a highest value and then decrease. In the numerical simulations carried out, the largest relative energy dissipation $w_D = 8.1\%$ was obtained for $R_0/R_{int}^{DC} = 5$, $t_0/t_{tr} = 1$ and $t_I/t_{tr} = 1.7$. Higher values can be achieved, but they can never exceed the 50% obtained for a harmonic wave under the condition of electrical impedance matching.

6. Conclusions

The main conclusions of this study can be summarized as follows: (i) A PBE with linear response can be represented by a three-port system with one electrical and two mechanical interfaces or ports at which it can interact with external active or passive devices. (ii) As far as these interactions are concerned, and due to symmetry and reciprocity assumed, the properties of the PBE are defined by four elements of a 3×3 impedance matrix. (iii) Principal advantages of the three-port approach are, on the one hand, that results for different environments or uses can be derived without specifying the PBE, and, on the other hand, that the characteristics of a specific PBE can be derived without reference to its environment or use. (iv) For a lossless PBE constituting a part of an elastic bar and used for generation of harmonic waves, the electrical input power is partitioned equally between the energy fluxes associated with two waves generated in the bar. (v) The dissipation of power associated with the resistive part of the internal impedance of the PBE corresponds to the

sum of these energy fluxes. (vi) For a lossless PBE constituting a part of an elastic bar and used for damping of harmonic waves it has been shown that under the condition of electrical impedance matching half of the mechanical input power supplied by an incident wave is dissipated in the load impedance, and one quarter of it is made up of the energy fluxes associated with each of the reflected and transmitted waves. (vii) In the equivalent electrical circuit, the dissipation of power in the resistive part of the internal impedance of the PBE corresponds to the sum of these energy fluxes. (viii) A PBE with its electrical port shunted by a load impedance can be represented as a system with two mechanical ports. (ix) In numerical simulations of damping of a bell-shaped wave, the highest fraction of the wave energy dissipated was 8.1%. (x) Higher relative energy dissipation can be achieved, but it cannot exceed the 50% obtained for a harmonic wave under condition of electrical impedance matching.

Acknowledgement

The authors gratefully acknowledge the economical support they have received from the Swedish Research Council (contract No. 621-2001-2156).

Appendix A. Derivation of the impedance matrix for the laminated PBE

The constitutive equations of the material of the piezoelectric layers a can be written as

$$\hat{e} = \frac{1}{E_a}\frac{\hat{N}_a}{A_a} - d_a\frac{\hat{U}_0}{h_a}, \quad \hat{D}_a = -d_a\frac{\hat{N}_a}{A_a} + \varepsilon_a\frac{\hat{U}_0}{h_a}, \tag{A.1}$$

where $\hat{e}(x,\omega)$ is the strain, $\hat{D}_a(x,\omega)$ is the electric displacement and $\hat{N}_a(x,\omega)$ is the normal force acting in each piezoelectric layer. Those of the materials of the bonding layers b and the core c are

$$\hat{e} = \frac{1}{E_b}\frac{\hat{N}_b}{A_b}, \quad \hat{e} = \frac{1}{E_c}\frac{\hat{N}_c}{A_c}, \tag{A.2a,b}$$

where $\hat{N}_b(x,\omega)$ and $\hat{N}_c(x,\omega)$ are the normal forces acting in these layers.

The charge on the electrodes of each piezoelectric layer is

$$\hat{Q}_a = \int_{-l/2}^{l/2} \hat{D}_a w_a \,\mathrm{d}x. \tag{A.3}$$

The current into the electrodes of the two piezoelectric layers is

$$\hat{i}_0 = 2\mathrm{i}\omega\hat{Q}_a. \tag{A.4}$$

Elimination of $\hat{Q}_a$, $\hat{D}_a$ and $\hat{U}_0$ from Eqs. (A.1), (A.3) and (A.4) gives

$$\hat{N}_a - k_a^2\hat{N}_a^{\mathrm{av}} = A_a E_a\left(\hat{e} + \frac{1}{2}\frac{d_a}{h_a}Z_a^E\hat{i}_0\right), \tag{A.5}$$

where $\hat{N}_a^{\mathrm{av}} = (1/l)\int_{-l/2}^{l/2}\hat{N}_a\,\mathrm{d}x$ is the average of $\hat{N}_a$ over the length l of the PBE.

Compatibility requires

$$\hat{e} = \frac{1}{\mathrm{i}\omega}\frac{\partial\hat{v}}{\partial x}, \tag{A.6}$$

where $\hat{v}(x,\omega)$ is the particle velocity. Substitution of Eq. (A.6) into Eq. (A.5) and averaging gives

$$(1-k_a^2)\hat{N}_a^{\mathrm{av}} = Z_a^M(\hat{v}_2 - \hat{v}_1) + \frac{1}{2}A_a E_a\frac{d_a}{h_a}Z_a^E\hat{i}_0. \tag{A.7}$$

The equation of axial motion is

$$\frac{\partial\hat{N}}{\partial x} = A\rho\mathrm{i}\omega\hat{v}, \tag{A.8}$$

where

$$\hat{N} = 2\hat{N}_a + 2\hat{N}_b + \hat{N}_c \tag{A.9}$$

is the total normal force. Elimination of $\hat{N}_a, \hat{N}_b$ and $\hat{N}_c$ by using Eqs. (A.2), (A.5) and (A.7) gives,

$$\hat{N} = \frac{AE}{\mathrm{i}\omega}\frac{\partial \hat{v}}{\partial x} + \alpha(\hat{v}_2 - \hat{v}_1) + \beta\hat{i}_0, \tag{A.10}$$

where

$$\alpha = 2\frac{k_a^2 Z_a^M}{1-k_a^2}, \quad \beta = A_a E_a \frac{d_a}{h_a}\frac{Z_a^E}{1-k_a^2}. \tag{A.11a,b}$$

Substituting Eq. (A.10) into Eq. (A.8) gives

$$\frac{\partial^2 \hat{v}}{\partial x^2} - \gamma^2 \hat{v} = 0. \tag{A.12}$$

The general solution of Eqs. (A.10) and (A.12) can be expressed as

$$\hat{N} = \hat{N}_p \mathrm{e}^{-\gamma x} + \hat{N}_n \mathrm{e}^{\gamma x} + \alpha(\hat{v}_2 - \hat{v}_1) + \beta\hat{i}_0, \tag{A.13a}$$

$$\hat{v} = \frac{1}{Z_{\mathrm{ch}}^M}(-\hat{N}_p \mathrm{e}^{-\gamma x} + \hat{N}_n e^{\gamma x}). \tag{A.13b}$$

Substituting this general solution into the boundary conditions

$$\hat{N}(-l/2,\omega) = \hat{N}_1(\omega), \quad \hat{v}(-l/2,\omega) = \hat{v}_1(\omega), \tag{A.14a,b}$$

$$\hat{N}(l/2,\omega) = \hat{N}_2(\omega), \quad \hat{v}(l/2,\omega) = \hat{v}_2(\omega) \tag{A.14b,c}$$

and eliminating $\hat{N}_p$ and $\hat{N}_n$ gives the normal forces

$$\hat{N}_1 = \beta\hat{i}_0 - \left(\alpha + \frac{Z_{\mathrm{ch}}^M}{\tanh(\gamma l)}\right)\hat{v}_1 + \left(\alpha + \frac{Z_{\mathrm{ch}}^M}{\sinh(\gamma l)}\right)\hat{v}_2 \tag{A.15a}$$

$$\hat{N}_2 = \beta\hat{i}_0 - \left(\alpha + \frac{Z_{\mathrm{ch}}^M}{\sinh(\gamma l)}\right)\hat{v}_1 + \left(\alpha + \frac{Z_{\mathrm{ch}}^M}{\tanh(\gamma l)}\right)\hat{v}_2 \tag{A.15b}$$

at the mechanical interfaces. Eqs. (A.1b), (A.3) and (A.4) give the current

$$\hat{i}_0 = \frac{2}{Z_a^E}\left(\hat{U}_0 - \frac{d_a h_a}{\varepsilon_a A_a}\hat{N}_a^{\mathrm{av}}\right), \tag{A.16}$$

at the electrical interface. Substituting $\hat{N}_a^{\mathrm{av}}$ from Eq. (A.7) into this relation gives the voltage

$$\hat{U}_0 = \frac{1}{2}\frac{Z_a^E}{1-k_a^2}\hat{i}_0 + \frac{d_a h_a}{\varepsilon_a A_a}\frac{Z_a^M}{1-k_a^2}(-\hat{v}_1 + \hat{v}_2) \tag{A.17}$$

at the electrical interface. Comparison of Eqs. (A.15) and (A.17) with Eq. (1) finally gives the elements of the impedance matrix **Z** according to Eqs. (2) and (4).

References

[1] G. Gautschi, *Piezoelectric Sensorics*, Springer, Berlin/Heidelberg, 2002.

[2] R.M. Lec, Piezoelectric biosensors: recent advances and applications, IEEE International Frequency Control Symposium and PDA Exhibition, 2001.

[3] J.K. Dürr, R. Honke, M. von Alberti, R. Sippel, Development of an adaptive lightweight mirror for space application, *Smart Materials and Structures* 12 (2003) 1005–1016.

[4] K.K. Tan, S.C. Ng, S.N. Huang, Assisted reproduction system using piezo actuator, 2004 International Conference on Communications, Circuits and Systems, IEEE Cat. No. 04EX914, Vol. 2(pt. 2), 2004, pp. 1200–1203.

[5] T. Ikeda, *Fundamentals of Piezoelectricity*, Oxford University Press, New York, 1990.
[6] E.F. Crawley, J. de Luis, Use of piezoelectric actuators as elements of intelligent structures, *AIAA Journal* 25 (10) (1987) 1373–1385.
[7] J. Pan, C.H. Hansen, S.D. Snyder, A study of the response of a simply supported beam to excitation by a piezoelectric actuator, *Journal of Intelligent Material Systems and Structures* 3 (1) (1992) 3–16.
[8] N.W. Hagood, W.H. Chung, A. von Flotow, Modelling of piezoelectric actuator dynamics for active structural control, *Journal of Intelligent Material Systems and Structures* 1 (3) (1990) 327–354.
[9] R.P. Thornburgh, A. Chattopadhyay, Simultaneous modeling of mechanical and electrical response of smart composite structures, *AIAA Journal* 40 (8) (2002) 1603–1610.
[10] R.P. Thornburgh, A. Chattopadhyay, A. Ghoshal, Transient vibration of smart structures using a coupled piezoelectric-mechanical theory, *Journal of Sound and Vibration* 274 (2004) 53–72.
[11] N.W. Hagood, A. von Flotow, Damping of structural vibrations with piezoelectric materials and passive electrical networks, *Journal of Sound and Vibration* 146 (1991) 243–268.
[12] S.O. Reza Moheimani, A survey of recent innovations in vibration damping and control using shunted piezoelectric transducers, *IEEE Transactions on Control Systems Technology* 11 (4) (2003) 482–494.
[13] M. Panella, G. Martinelli, RC distributed circuits for vibration damping in piezo-electromchanical beams, *IEEE Transactions on Circuits and Systems—II: Express Briefs* 52 (8) (2005) 486–490.
[14] A. Jansson, B. Lundberg, Piezoelectric generation of extensional waves in a viscoelastic bar by use of a linear power amplifier: theoretical basis, *Journal of Sound and Vibration* 306 (2007) 318–332.
[15] A. Jansson, U. Valdek, B. Lundberg, Generation of prescribed waves in an elastic bar by use of piezoelectric actuators driven by a linear power amplifier, *Journal of Sound and Vibration* 306 (2007) 751–765.
[16] P. Nauclér, B. Lundberg, T. Söderström, A mechanical wave diode: using feedforward control for one-way transmission of elastic extensional waves, *IEEE Transactions on Control Systems Technology* 15 (4) (2007).
[17] A. Jansson, B. Lundberg, Damping of elastic strain waves by means of a piezoelectric bar element feeding an external RL circuit, *Journal of Sound and Vibration* (2008), doi:10.1016/j.jsv.2007.12.033.
[18] C. Coleman, *An Introduction to Radio Frequency Engineering*, Cambridge University Press, Cambridge, 2004.